Since January 2020 Elsevier has created a COVID-19 resource centre with free information in English and Mandarin on the novel coronavirus COVID-19. The COVID-19 resource centre is hosted on Elsevier Connect, the company's public news and information website.

Biochimica et Biophysica Acta 1828 (2013) 2026–2031

Contents lists available at SciVerse ScienceDirect

Biochimica et Biophysica Acta

journal homepage: www.elsevier.com/locate/bbamem

Analysis of SARS-CoV E protein ion channel activity by tuning the protein and lipid charge

Carmina Verdiá-Báguena [a], Jose L. Nieto-Torres [b], Antonio Alcaraz [a], Marta L. DeDiego [b], Luis Enjuanes [b], Vicente M. Aguilella [a,*]

[a] Department of Physics, Laboratory of Molecular Biophysics, Universitat Jaume I, 12071 Castellón, Spain
[b] Department of Molecular and Cell Biology, Centro Nacional de Biotecnología (CNB-CSIC), Campus Universidad Autónoma de Madrid, Darwin 3, 28049 Madrid, Spain

ARTICLE INFO

Article history:
Received 9 January 2013
Received in revised form 24 April 2013
Accepted 9 May 2013
Available online 18 May 2013

Keywords:
Coronavirus
Ion channel
Lipid charge
Envelope protein
SARS

ABSTRACT

A partial characterization of the ion channels formed by the SARS coronavirus (CoV) envelope (E) protein was previously reported (C. Verdiá-Báguena et al., 2012 [12]). Here, we provide new significant insights on the involvement of lipids in the structure and function of the CoV E protein channel on the basis of three series of experiments. First, reversal potential measurements over a wide range of pH allow the dissection of the contributions to channel selectivity coming from ionizable residues of the protein transmembrane domain and also from the negatively charged groups of diphytanoyl phosphatidylserine (DPhPS) lipid. The corresponding effective pKas are consistent with the model pKas of the acidic residue candidates for titration. Second, the change of channel conductance with salt concentration reveals two distinct regimes (Donnan-controlled electrodiffusion and bulk-like electrodiffusion) fully compatible with the outcomes of selectivity experiments. Third, by measuring channel conductance in mixtures of neutral diphytanoyl phosphatidylcholine (DPhPC) lipids and negatively charged DPhPS lipids in low and high salt concentrations we conclude that the protein–lipid conformation in the channel is likely the same in charged and neutral lipids. Overall, the whole set of experiments supports the proteolipidic structure of SARS-CoV E channels and explains the large difference in channel conductance observed between neutral and charged membranes.

1. Introduction

Coronaviruses are enveloped viruses that cause common colds in humans and other serious diseases in birds and mammals [1]. One of these coronaviruses is responsible for the severe acute respiratory syndrome (SARS-CoV), which, between 2002 and 2003, affected 8000 people worldwide and resulted lethal in the 10% of the cases. All coronaviruses express the envelope (E) protein, a multifunctional short polypeptide involved in virus morphogenesis and virulence [2–5]. SARS-CoV E protein is 76 amino acid long and contains an alpha-helical transmembrane (TM) domain that spans the lipid membrane with ~28 residues [6] (Fig. 1) SARS-CoV E protein oligomerizes forming a pentameric structure that displays ion channel activity [7–12] a remarkable function for this protein that may affect virus host interaction.

In a recent paper [12] we reported that SARS-CoV E protein channels (as well as a synthetic peptide representing just the protein TM) exhibit different functional properties when reconstituted in neutral or charged planar lipid membranes. This data suggested that lipid molecules likely assemble with E protein oligomers to form a combined proteolipidic structure. In this structure the lipids could be only located at the channel entrances, or alternatively, within the lipid polar heads, stabilized by peptides, lining totally or partially the pore wall. The ion channel activity of a number of transmembrane proteins, as well as of small peptides and antimicrobial peptides, is strongly dependent on the lipid environment [13,14]. Actually, evidence on the lipid involvement in the channel structure is often obtained from the sensitivity of the pore-forming activity to the curvature of the lipid bilayer membranes [15]. The reason for that lies in the high energy cost of assembling lipidic structures in membranes with intrinsic curvature that usually inhibits the channel activity [16]. In this sense, we observed a lower probability of pore formation by SARS-CoV E protein in membranes containing phosphatidylethanolamine (DOPE), a lipid with negative intrinsic curvature [12], which suggests a significant involvement of lipid molecules in channel structure.

However, the correlation between the pore forming potency of peptides and the spontaneous curvature of the lipid is not a definitive argument to elucidate the actual structure of the SARS-CoV E channels. Similar correlations have been reported in well-known proteinaceous pores like alamethicin. In this case, the sensitivity of the channel to the lipid charge comes from a peptide-induced membrane thinning [13,17]. Therefore, in the case of SARS-CoV E protein, it seems important to obtain additional lines of evidence on the mechanism of pore formation and the functional properties of the resulting ion channels [12].

* Corresponding author. Tel.: +34 964728045; fax: +34 964729218.
E-mail address: aguilell@uji.es (V.M. Aguilella).

0005-2736/$ – see front matter
http://dx.doi.org/10.1016/j.bbamem.2013.05.008

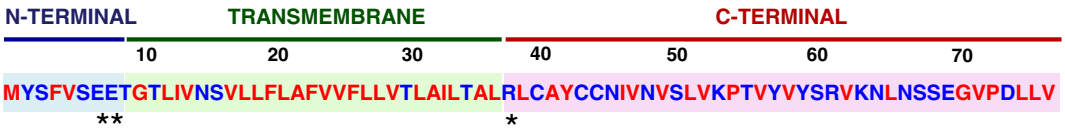

Fig. 1. SARS-CoV E protein sequence. E protein is divided into three domains: the amino terminal (N-terminal), the transmembrane and the carboxy terminal (C-terminal). Red letters represent hydrophobic amino acids, and blue letters indicate hydrophilic amino acids. Asterisks highlight polar charged amino acids located at the beginning (two glutamic acid residues) and at the end (an arginine) of the transmembrane domain, respectively.

To address these issues a different strategy has been adopted in this manuscript, which is complementary to other structural studies [7]. We generated useful information on the CoV E channel structure by focusing on the effect of lipid charge on channel conductance and ionic selectivity under a variety of conditions. Several series of experiments are reported that have in common the modulation of the effective protein and lipid charge presented to the small ions crossing the aqueous pore [18]. First, reversal potential measurements under different pH conditions enabled us to identify the contributions of ionizable residues of the protein TM and also of the negatively charged groups of DPhPS lipid to channel selectivity. Secondly, the change of channel conductance in membranes containing varying ratios of neutral DPhPC lipids and charged DPhPS lipids in low and high salt concentrations was studied. Finally, protein and lipid charges were modified by changing the salt concentration of the solution both in neutral and charged membranes and the corresponding channel conductance and the solution conductivity were determined.

These three ways of modifying the effective fixed charge in CoV E channels strongly supported a proteolipidic structure of the channel that is likely to be the same in charged and neutral membranes. In other words, if this assumption proves correct, the large difference (two-fold change) between channel conductance in 1 M KCl in DPhPS and DPhPC host membranes would be simply an effect of the partial Donnan exclusion of anions in the aqueous pore [19].

Overall, exploring the lipid charge effects on channel conductance and selectivity over a wide range of lipid compositions, salt concentration and solution pH provided a unitary message for the protein–lipid composition of the channel. The results supported a proteolipidic structure without the need of additional sophisticated structural techniques.

2. Materials and methods

2.1. Protein synthesis

Full-length SARS-CoV E protein was kindly provided by Dr. Jaume Torres and synthesized and purified as previously described [12].

2.2. Ion channel reconstitution and ionic current recording

Planar bilayers were formed by apposition of two monolayers prepared from a solution of 1% pure diphytanoyl phosphatidylcholine (DPhPC), pure diphytanoyl phosphatidylserine (DPhPS), or a mixture of both lipids (Avanti polar lipids, Inc., Alabaster, AL) in pentane. Lipids were added on 70–90 μm diameter orifices in the 15 μm-thick Teflon partition that separated two identical chambers [20,21]. The orifices were pretreated with a 1% solution of hexadecane in pentane. Aqueous solutions of KCl were buffered with 5 mM HEPES at pH 6. All measurements were performed at room temperature (23 ± 1 °C). Ion channel insertion was achieved by adding 0.5–1 μl of a 300 μg/ml solution of synthetic protein in the buffer containing acetonitrile:isopropanol (40:60) on one side of the chamber (hereafter referred to as *cis* side).

An electric potential was applied using Ag/AgCl electrodes in 2 M KCl, 1.5% agarose bridges assembled within standard 250 μl pipette tips. The potential was defined as positive when it was higher on the side of the peptide addition (*cis* side), whereas the *trans* side was set to ground. An Axopatch 200B amplifier (Molecular Devices, Sunnyvale, CA) in the voltage-clamp mode was used to measure the current and the applied potential. The chamber and the head stage were isolated from external noise sources with a double metal screen (Amuneal Manufacturing Corp., Philadelphia, PA). The channel conductance was obtained from current measurements under an applied potential of +100 mV in symmetrical salt solutions of variable KCl concentration. The conductance values were evaluated using the Gaussian fit tool of Sigma Plot 10.0 (Systat Software, Inc.).

The reversal potential, E_{rev}, was obtained as follows. First, a lipid membrane was formed at a given salt concentration gradient. Second, one or several channels were inserted into the bilayer and a net ionic current appeared due to the concentration gradient. Third, the ionic current through the channel was manually set to zero by adjusting the applied potential. The potential needed to achieve zero current was then corrected by the liquid junction potentials of the electrode salt bridges [22] to obtain the E_{rev}.

3. Results and discussion

3.1. Ion channel activity in planar lipid bilayers

The spontaneous formation of full-length SARS-CoV E protein ion channels in DPhPC and DPhPS membranes as well as their current recording did not show significant differences to the analogous process done previously for synthetic peptides derived from the SARS-CoV E protein TM domain [12]. The reversal potential was measured in multichannel experiments as the voltage required to null the ionic current. To estimate the most probable value of channel conductance, we recorded more than 40 long duration (~200 s each) current traces and made a statistical analysis of all the current jump events, including positive (increase) and negative (decrease) bursts.

Fig. 2 shows typical current traces recorded in DPhPC membranes (panel A) and DPhPS membranes (panel C) of SARS-CoV E channel. As already observed in electrophysiological measurements with synthetic peptides [12], CoV E channels formed in DPhPS membranes showed a better defined conductance (190 ± 60 pS), compared with channels formed in DPhPC membranes, which exhibited a higher dispersion in the magnitude of the current bursts (370 ± 160 pS). This trend can be clearly observed in the histograms included in Fig. 2. The origin of this different conductance variability depending on the host lipid remains unexplained.

3.2. Channel selectivity change with pH

The SARS-CoV E channel was reported to be slightly cationic selective in negatively charged membranes and almost non-selective in neutral membranes at pH 6 [8,12]. From those results it became apparent the large influence of the lipid charge on the channel preference for cations. To further analyze this effect, channel selectivity in solutions of varying acidity was measured using the same concentration gradient used in previous studies (500 mM *cis*|50 mM *trans*). Two series of reversal potential measurements were performed over a wide range of pH (1.5–7): first in neutral membranes (DPhPC) and then, using negatively charged membranes (DPhPS). The channel selectivity was strongly dependent on the net charge of the host lipid (Fig. 3). When reconstituted in DPhPC, the channel displayed a very

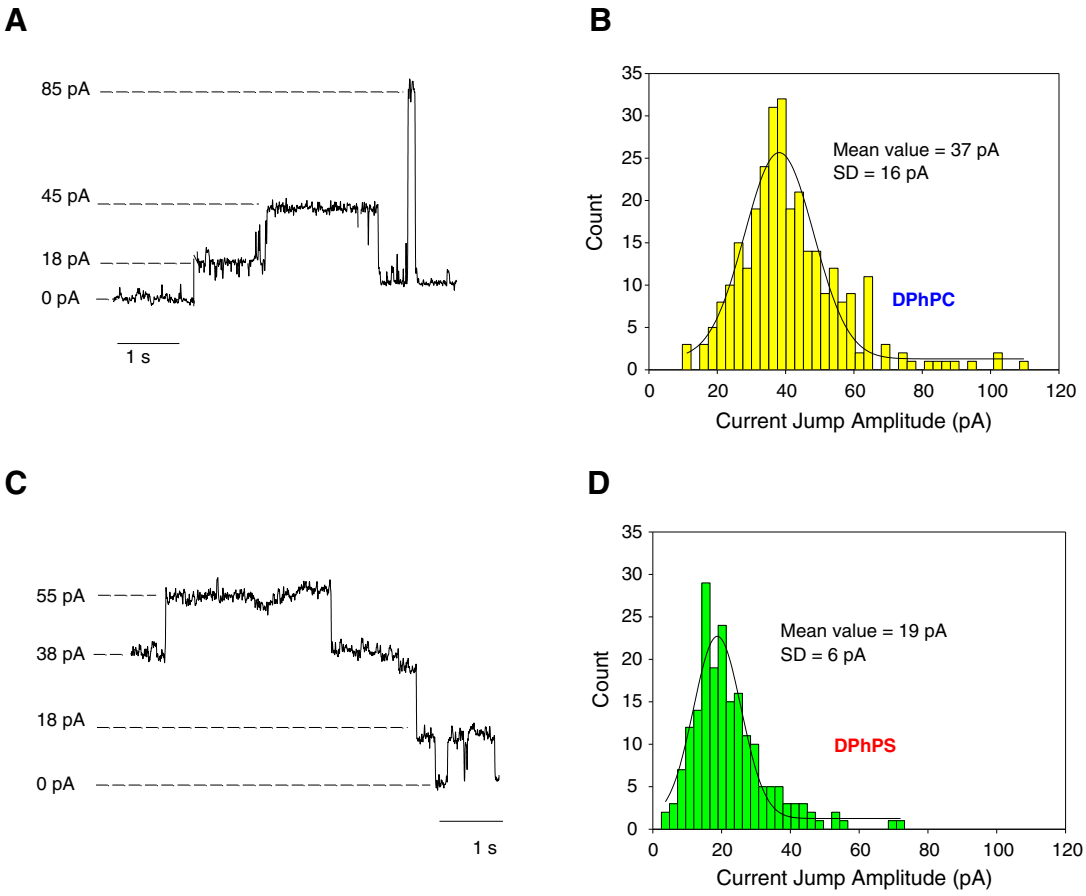

Fig. 2. SARS-CoV E channel current recordings and histograms of the current jump amplitude in 1 M KCl at pH 6. A and B: Traces and histogram of channels formed in pure DPhPC. C and D: Traces and histogram of channels formed in pure DPhPS. As the corresponding histograms show, the current jump levels in DPhPS membranes are more well-defined than in DPhPC where a larger variety of current jump amplitudes are recorded. Data were fitted to a single Gaussian. Mean values and standard deviations were 370 ± 160 pS in DPhPC and 190 ± 60 pS in DPhPS.

mild cationic selectivity at neutral pH (ratio of the permeability to positive versus negative ions, $P_+/P_- = 1 \pm 0.1$) and a moderate anionic selectivity in highly acidic solutions (pH 1.5) ($P_+/P_- = 0.3 \pm 0.1$). This change may be attributed to the protonation of some ionizable residues of the CoV E protein TM domain.

However, when the channels were inserted in DPhPS membranes, the change in selectivity from pH 6 to pH 1.5 was much more significant and titration of charges even reversed the channel selectivity from cationic selectivity to anionic one.

The reversal potential measurements performed in DPhPC membranes displayed the typical one-site titration trend seen in other channels [18,23–27]. We have fitted this set of E_{rev} values to Eq. (1), similar to the standard sigmoidal dose–response curves.

$$E_{rev} = E_{\min} + \frac{E_{\max} - E_{\min}}{1 + 10^{pH - pKa1}} \quad (1)$$

The low pH ($E_{\max}$) and neutral pH ($E_{\min}$) values for E_{rev} were taken from the experimental data and pKa1 was the only fitting parameter. This approach has been successfully used in other weakly selective ion channels [23,24,28]. The best fit (solid line of upper plot in Fig. 3) corresponds to pKa1 = 4.3, a value that is close to the model pKa of glutamate, one of the charged residues of the TM domain of SARS-CoV E protein. Actually, the amino acid sequence of that domain contains only two negative residues near the amino terminus: E7 and E8.

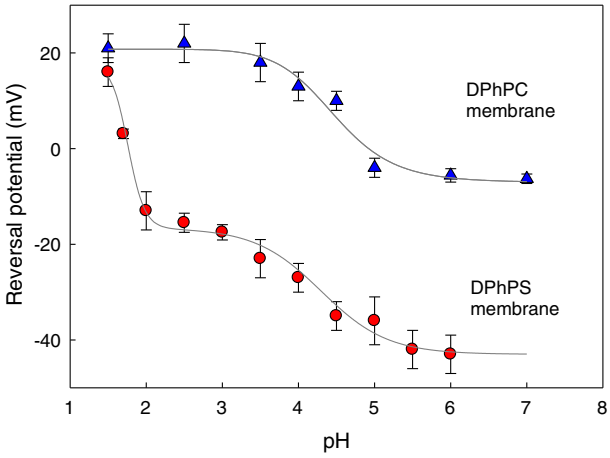

Fig. 3. E protein channel titration. Reversal potential was measured for SARS-CoV E protein channels in neutral DPhPC membranes (triangles) and negatively charged DPhPS membranes (circles). Under the conditions of the experiments (500 mM KCl *cis*|50 mM KCl *trans*), negative and positive reversal potentials imply cationic and anionic selectivity, respectively. The lipid charge is the main determinant of channel ion selectivity but the subsequent titration of negative groups eventually switches the cationic selectivity into anionic in a high acidity medium, regardless of the nature of the host lipid. Solid lines denote the best fit of the data according to Eq. (1) (top plot) and Eq. (2) (bottom plot). Each point is the average of measurements in 10–15 channels.

The series of E_{rev} measurements in DPhPS membranes (red circles in Fig. 3) cannot be fitted to a classical one-site titration curve. We have slightly modified Eq. (1) to account for the double transition observed in selectivity and we have used Eq. (2):

$$E_{rev} = E_{\min} + \frac{E_{int} - E_{\min}}{1 + 10^{pH-pKa1}} + \frac{E_{\max} - E_{int}}{1 + 10^{pH-pKa2}}. \quad (2)$$

By taking the low pH ($E_{\max}$) and neutral pH ($E_{\min}$) values for E_{rev} from the experimental data and leaving pKa1 and pKa2 as well as E_{int} as fitting parameters, the best fit was obtained for $E_{int} = -19$ mV, pKa1 = 4.3 and pKa2 = 1.73. The easiest interpretation of this second effective pKa seen in the titration curve is to ascribe this value to the carboxyl group of the PS polar head although titration of the phosphate group cannot be totally excluded. This would support the view that lipids line the pore lumen and not only contribute but also determine the channel selectivity. The model pKas of serine carboxyl group reported in the literature are in the range 2.5–4.5 [29,30]. However, when the ionization occurs in confined spaces as the pore, where protons see a different electric potential near the ionizable site, it is expected a significant deviation from the model pKa [30]. In concentrated solutions the apparent pKa (the one obtained from titration curves) should be shifted towards lower values [31]. Interestingly, the fitting value of pKa1 = 4.3 is the same in both series of measurements. This fact may indicate that the protonation of glutamates in the TM protein domain is not affected by the presence of carboxyl groups of the lipid polar heads despite the presumably tight arrangement of the TM helices and the lipid molecules. This is consistent with the fact that there are many more carboxyl than glutamate groups lining the pore so that the organization of helices and lipid molecules in the pore may be such that both types of charged groups are kept apart from each other.

The reversal potential measurements for both kinds of lipids (DPhPC and DPhPS) are almost equal in solutions of high acidity. This implies that the channel preference for Cl^- ions over K^+ ions at pH ~1.5 is the same no matter whether the pore structure includes PC or PS lipids. Bearing in mind that lipid polar heads are neutral at such low pH, this anionic selectivity can only arise from positively charged residues of the TM helices like arginine R38. This suggests that the charge of the lipid heads does not necessarily change the structural conformation of the aqueous pore: the spatial distribution of positive residues in the channel could be similar when the protein channel is formed either in DPhPC or DPhPS membranes.

3.3. Conductance is strongly dependent on the net charge of the host lipid

In a recent study [12], we reported that the conductance of SARS-CoV E protein channel in 1 M KCl and pH 6 was $G = 370 \pm 160$ pS in DPhPC membranes and $G = 190 \pm 60$ pS in DPhPS membranes. These values raise relevant questions. The main one is how to interpret the result obtained for DPhPC that is almost twice the value obtained for DPhPS. This, together with huge standard deviations found in the experiments could question whether the unitary channel conductance reported in neutral membranes is truly a single-channel conductance or it is the result of two simultaneous insertion events. To address this issue, we measured channel conductance in membranes with variable lipid composition between pure DPhPC and pure DPhPS. The values of channel conductance were extracted from the histograms of current jump amplitudes. Both new insertions as well as channel closures were considered as events for the statistics [12]. The experimental results in 1 M KCl solutions and pH 6 are shown at the top panel of Fig. 4 (circles). There is a smooth transition from 370 pS (DPhPC membranes) to 190 pS (DPhPS membranes) and the channel conductance decreases with the mass percentage of DPhPS lipid. This result clearly supports the interpretation already given in the preliminary version of these experiments [12], confirming that the channel conductance in 1 M KCl decreases as the charge of the lipid increases (Fig. 4).

This directly leads to the next question. According to intuitive electrostatic arguments, the accumulation of ions near the pore entrance due to the lipid charge should give just the opposite effect, i.e. greater channel conductance in DPhPS. Thus, we may ask whether the difference in conductance requires more elaborated arguments or if it could just be explained by a change in the aqueous pore size caused by a different lipid–protein conformation. A new series of conductance measurements performed in membranes of variable composition using diluted KCl solutions (30 mM) could shed some light on this issue. The experiments reported at the bottom panel of Fig. 4 (triangles) show that channel conductance in neutral membranes is lower (almost one third) than in fully charged membranes, exactly opposite to what was observed in concentrated salt solutions. If the changes in conductance with the lipid composition were simply a consequence of different protein–lipid conformations yielding changes in the pore size, the ionic current should decrease or increase in a similar way at low and high salt concentrations. Although a change in the pore size between DPhPC and DPhPS membranes cannot be categorically excluded, the main cause for this large change in channel conductance between them must be sought elsewhere.

3.4. Change of channel conductance with salt concentration

A classical way of analyzing the transport properties of a membrane channel is to compare channel conductance and bulk solution conductivity change at different salt concentrations [32,33]. The relation between channel conductance versus bulk solution conductivity for a wide range of salt concentration (30 mM–1.5 M KCl) at pH 6 was determined (Fig. 5).

In neutral membranes, channel conductance changes linearly with solution conductivity (the slope of the double logarithmic plot is very close to unity). This means that the interaction between the permeating ions and the channel is so weak that ion conduction in the pore and in bulk solution is pretty similar to each other. This is consistent with the weak selectivity of the channel at neutral pH (see Fig. 3, top plot) [12]. The channel resembles a neutral nanopore and ion permeation is barely influenced by the low fixed charge density in the protein TM domain. In contrast, when channel conductance is measured in DPhPS membranes, two distinct regimes were observed. In low concentration solutions (30–100 mM KCl), channel conductance is ~70 pS and is independent of conductivity. In contrast, in more concentrated solutions (0.3–1.5 M KCl) conductance increases with conductivity but does not scale with bulk conductivity, as it is the case in charged pores [14]. This result

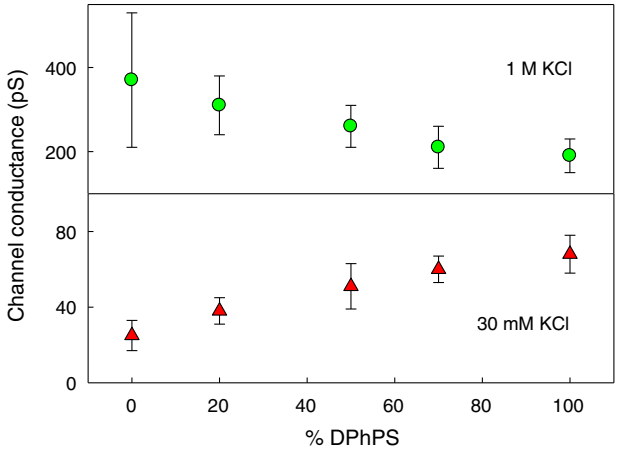

Fig. 4. Channel conductance for SARS-CoV E protein in different lipid compositions and salt concentration. E protein conductance in planar membranes made of different mixtures of neutral DPhPC and negatively charged DPhPS lipids in 1 M KCl (top panel) and 30 mM KCl solutions (bottom panel) at pH 6. For clarity, the vertical axis scaling is different in each panel. The fraction of charged lipid is given in mass percentage.

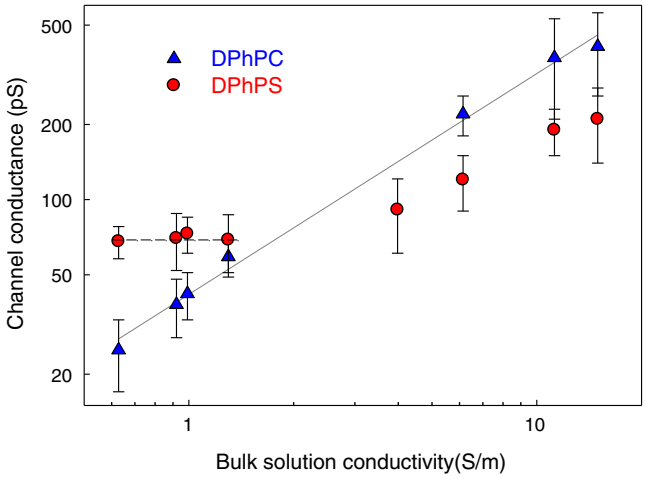

Fig. 5. Double logarithmic plot of channel conductance of the SARS-CoV E versus bulk solution conductivity. Channel conductance in DPhPC (triangles) is proportional to bulk solution conductivity. However, in DPhPS (circles), conductance is independent from conductivity in low concentration KCl solutions (30–100 mM) but increases with conductivity in more concentrated solutions (0.3–1.5 M).

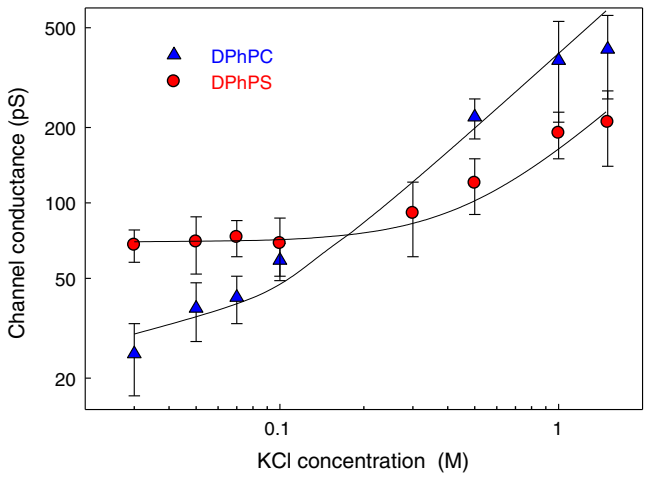

Fig. 6. Channel conductance of SARS-CoV E protein channel in neutral DPhPC (triangles) and negatively charged DPhPS (circles) at pH 6. In DPhPS membranes and low concentration KCl solutions (30–100 mM) the channel conductance remains unaltered because the ionic concentration within the pore is controlled by the channel fixed charge. In more concentrated solutions (0.3–1.5 M), the conductance increases with the bulk KCl concentration following fairly well the dependence given by Eq. (4).

is in line with the cationic selectivity of the CoV E channel in negatively charged membranes (see Fig. 3, bottom plot) and with the fact that the preference for K^+ ions should be reflected on the channel conductance, particularly when KCl concentration is smaller than the effective negative fixed charge concentration in the pore.

To go a step further of this qualitative explanation of the conductance vs. conductivity dependence in neutral and charged membranes, we assumed that channel conductance is proportional to the total concentration of mobile ions inside the channel, i.e. $G \propto (c_+ + c_-)$ and the K^+ and Cl^- average concentrations inside the pore were calculated by using Donnan equilibrium equations [18].

$$c_+ = -\rho/2 + \left(c^2 + \rho^2/4\right)^{1/2}$$
$$c_- = \rho/2 + \left(c^2 + \rho^2/4\right)^{1/2} \quad (3)$$

where c is the salt bulk concentration and ρ is the average fixed charge concentration inside the channel (with the corresponding sign). Then, conductance was normalized to the lowest value (the one measured in 30 mM KCl) and ρ was regarded as a fitting parameter:

$$G(c)/G(30\text{mM}) = \left(c^2 + \rho^2/4\right)^{1/2}. \quad (4)$$

The best fits of the conductance vs. concentration dependence were determined (Fig. 6, solid lines). For the series of measurements in DPhPC $\rho = 0.14$ M. For conductance values in DPhPS $\rho = 0.94$ M. Despite the simplicity of the theory invoked, both values give accurate fits of the respective measurements and are consistent with the change of conductance with solution conductivity. In DPhPC, only the negative residues of the protein TM domain contribute to the fixed charge concentration and their effect is of minor importance. In DPhPS membranes, as long as the bulk concentration is smaller than ρ, the ion concentration inside the pore rises to match ρ so that local electroneutrality is ensured. Charge neutrality is then the reason why in this regime, channel conductance is higher than in a neutral pore and almost independent of bulk concentration. When bulk concentration becomes comparable to ρ, counterions (ions of opposite charge to ρ) accumulate and coions (ions with the same charge as ρ) are excluded following Donnan equilibria. Finally, when salt concentration is much greater than ρ, Donnan exclusion comes to be negligible and conductance increases almost linearly with the total ion concentration in the pore, similarly to a neutral pore.

The values obtained for the average fixed charge concentration in the pore are also consistent with the difference in reversal potential measured at pH 6 in DPhPC and DPhPS membranes. Although we cannot exclude completely a different arrangement of protein helices and lipid molecules in neutral and charged membranes, our experiments provide strong evidence that the charged groups within the pore can account by themselves for the higher ionic current measured in charged membranes.

4. Concluding remarks

Novel insights on the involvement of lipids in the structure and function of the CoV E protein channel are presented here by analyzing the reconstituted ion channels in artificial membranes under a variety of different conditions. On one side, reversal potential experiments indicate that although both the protein and the lipid charges participate in the overall ionic selectivity of the pore, they play separate roles that can be clearly dissected. On the other side, channel conductance measurements suggest that the lipid charges contribute to the channel current by accumulating counterions as described by the well-known Donnan equilibrium. However, this simple effect must be handled with care because it leads to distinct regimes depending on the balance between the bulk electrolyte concentration and the average fixed charge concentration inside the channel. Interestingly, both kinds of experiments performed in neutral and charge lipids can be rationalized with no need to appeal to different channel conformations. This does not exclude the existence of different protein–lipid conformations, but stresses how important is the understanding of charge regulation effects that otherwise could be mistakenly attributed to changes in pore size.

Acknowledgements

This work was supported by grants from the Ministry of Science and Innovation of Spain (MICINN. FIS2010-19810, BIO2007-60978 and BIO2010-16705), Fundació Caixa Castelló-Bancaixa (P1-1B2012-03), Generalitat Valenciana (Prometeu/2012/069), the European Community's Seventh Framework Programme (FP7/2007–2013) under the project "EMPERIE" EC grant agreement number 223498, and the U.S. National Institutes of Health (NIH) (2P01AI060699-06A1, W000306844). CVB received a fellowship from UJI. JLN received a fellowship from CSIC. We thank Jaume Torres for providing reagents, and Marga Gonzalez for her technical assistance.

References

[1] L. Enjuanes, F. Almazán, I. Sola, S. Zuñiga, Biochemical aspects of coronavirus replication and virus–host interaction, Annu. Rev. Microbiol. 60 (2006) 211–230.
[2] J. Ortego, J.E. Ceriani, C. Patiño, J. Plana, L. Enjuanes, Absence of E protein arrests transmissible gastroenteritis coronavirus maturation in the secretory pathway, Virology 368 (2007) 296–308.
[3] M.L. DeDiego, E. Álvarez, F. Almazán, M.T. Rejas, E. Lamirande, A. Roberts, W.-J. Shieh, S.R. Zaki, K. Subbarao, L. Enjuanes, A severe acute respiratory syndrome coronavirus that lacks the E gene is attenuated in vitro and in vivo, J. Virol. 81 (2006) 1701–1713.
[4] M.L. DeDiego, L. Pewe, E. Alvarez, M.T. Rejas, S. Perlman, L. Enjuanes, Pathogenicity of severe acute respiratory coronavirus deletion mutants in hACE-2 transgenic mice, Virology 376 (2008) 379–389.
[5] M.L. DeDiego, J.L. Nieto-Torres, J.M. Jiménez-Guardeño, J.A. Regla-Nava, E. Álvarez, J.C. Oliveros, J. Zhao, C. Fett, S. Perlman, L. Enjuanes, Severe acute respiratory syndrome coronavirus envelope protein regulates cell stress response and apoptosis, PLoS Pathog. 7 (2011) e1002315.
[6] J.L. Nieto-Torres, M.L. DeDiego, E. Alvarez, J.M. Jiménez-Guardeño, J.A. Regla-Nava, M. Llorente, L. Kremer, S. Shuo, L. Enjuanes, Subcellular location and topology of severe acute respiratory syndrome coronavirus envelope protein, Virology 415 (2011) 69–82.
[7] K. Pervushin, E. Tan, K. Parthasarathy, X. Lin, F.L. Yu Jiang, D.A. Vararattanavech, T.W. Soong, D.X. Liu, J. Torres, Structure and inhibition of the SARS coronavirus envelope protein ion channel, PLoS Pathog. 5 (2009) e1000511.
[8] L. Wilson, C. McKinlay, P. Gage, SARS coronavirus E protein forms cation-selective ion channels, Virology 330 (2004) 322–331.
[9] J. Torres, J. Wang, K. Parthasarathy, D.X. Liu, The transmembrane oligomers of coronavirus protein E, Biophys. J. 88 (2005) 1283–1290.
[10] J. Torres, K. Parthasarathy, X. Lin, R. Saravanan, A. Kukol, D.X. Liu, Model of a putative pore: the pentameric α-helical bundle of SARS coronavirus E protein in lipid bilayers, Biophys. J. 91 (2006) 938–947.
[11] J. Torres, U. Maheswari, K. Parthasarathy, L. Ng, D. Xiang Liu, X. Gong, Conductance and amantadine binding of a pore formed by a lysine-flanked transmembrane domain of SARS coronavirus envelope protein, Protein Sci. 16 (2007) 2065–2071.
[12] C. Verdiá-Báguena, J.L. Nieto-Torres, A. Alcaraz, M.L. DeDiego, J. Torres, V.M. Aguilella, L. Enjuanes, Coronavirus E protein forms ion channels with functionally and structurally-involved membrane lipids, Virology 432 (2012) 485–494.
[13] A.A. Sobko, E.A. Kotova, Y.N. Antonenko, S.D. Zakharov, W.A. Cramer, Lipid dependence of the channel properties of a colicin E1-lipid toroidal pore, J. Biol. Chem. 281 (2006) 14408–14416.
[14] V.V. Malev, L.V. Schagina, P.A. Gurnev, J.Y. Takemoto, E.M. Nestorovich, S.M. Bezrukov, Syringomycin E channel: a lipidic pore stabilized by lipopeptide? Biophys. J. 82 (2002) 1985–1994.
[15] A.A. Sobko, E.A. Kotova, Y.N. Antonenko, S.D. Zakharov, W.A. Cramer, Effect of lipids with different spontaneous curvature on the channel activity of colicin E1: evidence in favor of a toroidal pore, FEBS Lett. 576 (2004) 205–210.
[16] S.M. Bezrukov, Functional consequences of lipid packing stress, Curr. Opin. Colloid Interface Sci. 5 (2000) 237–240.
[17] M.T. Lee, W.C. Hung, F.Y. Chen, H.W. Huang, Many-body effect of antimicrobial peptides: in the correlation between lipid's spontaneous curvature and pore formation, Biophys. J. 89 (2005) 4006–4016.
[18] A. Alcaraz, E.M. Nestorovich, M. Aguilella-Arzo, V.M. Aguilella, S.M. Bezrukov, Salting out the ionic selectivity of a wide channel: the asymmetry of OmpF, Biophys. J. 87 (2) (2004) 943–957.
[19] N. Lakshminarayanaiah, Equations of Membrane Biophysics, Academic Press, New York, 1984.
[20] S.M. Bezrukov, I. Vodyanoy, Probing alamethicin channels with water-soluble polymers. Effect on conductance of channel states, Biophys. J. 64 (1993) 16–25.
[21] M. Montal, P. Mueller, Formation of bimolecular membranes from lipid monolayers and a study of their electrical properties, Proc. Natl. Acad. Sci. U. S. A. 69 (1972) 3561–3566.
[22] A. Alcaraz, E.M. Nestorovich, M.L. López, E. García-Giménez, S.M. Bezrukov, V.M. Aguilella, Diffusion, exclusion, and specific binding in a large channel: a study of OmpF selectivity inversion, Biophys. J. 96 (2009) 56–66.
[23] J. Cervera, A.G. Komarov, V.M. Aguilella, Rectification properties and pH-dependent selectivity of Meningococcal class 1 porin, Biophys. J. 94 (2008) 1194–1202.
[24] T.K. Rostovtseva, T.-T. Liu, M. Colombini, V.A. Parsegian, S.M. Bezrukov, Positive cooperativity without domains or subunits in a monomeric membrane channel, Proc. Natl. Acad. Sci. U. S. A. 97 (2000) 7819–7822.
[25] L. Raymond, S.L. Slatin, A. Finkelstein, Channels formed by colicin E1 in planar lipid bilayers are large and exhibit pH-dependent ion selectivity, J. Membr. Biol. 84 (1975) 173–181.
[26] J.O. Bullock, Ion selectivity of colicin E1: modulation by pH and membrane composition, J. Membr. Biol. 125 (1992) 255–271.
[27] P.G. Merzlyak, M.P. Capistrano, A. Valeva, J.J. Kasianowicz, O.V. Krasilnikov, Conductance and ion selectivity of a mesoscopic protein nanopore probed with cysteine scanning mutagenesis, Biophys. J. 89 (2005) 3059–3070.
[28] A. Alcaraz, M. Queralt-Martín, E. García-Giménez, V.M. Aguilella, Increased salt concentration promotes competitive block of OmpF channel by protons, BBA Biomembr. 1818 (2012) 2777–2782.
[29] J.F. Tocanne, J. Teissie, Ionization of phospholipids and phospholipid-supported interfacial lateral diffusion of protons in membrane model systems, Biochim. Biophys. Acta 1031 (1990) 111–142.
[30] T.K. Rostovtseva, V.M. Aguilella, I. Vodyanoy, S.M. Bezrukov, V.A. Parsegian, Membrane surface-charge titration probed by gramicidin A channel conductance, Biophys. J. 75 (1998) 1783–1792.
[31] F.C. Tsui, D.M. Ojcius, W.L. Hubbel, The intrinsic pKa values for phosphatidylserine and phosphatidylethanolamine in phosphatidylcholine host bilayers, Biophys. J. 49 (1986) 459–468.
[32] B. Hille, Ion Channels of Excitable Membranes, 3rd ed. Sinauer, Sunderland, MA, 2001.
[33] F. Helfferich, Ion Exchange, McGraw-Hill, New York, 1962.